Rate of Access to the Binding Sites in Organically Modified Silicates. 1. Amorphous Silica Gels Grafted with Amine or Thiol Groups

Alain Walcarius,* Mathieu Etienne, and Jacques Bessière

Laboratoire de Chimie Physique et Microbiologie pour l'Environnement, Unité Mixte de Recherche UMR 7564, CNRS−Université H. Poincaré Nancy I, 405, rue de Vandoeuvre, F-54600 Villers-les-Nancy, France

Received January 16, 2002. Revised Manuscript Received March 21, 2002

The speed at which selected reactants are reaching active sites grafted on porous silica gels of various nature and porosity was evaluated using some model systems: protonation of aminopropyl-grafted silica (APS), mercury(II) binding on mercaptopropyl-grafted silica (MPS), and accumulation of copper(II) on APS. Data were obtained from batch experiments, by monitoring the consumption of reactant in solutions containing the solid phases as dispersed particles (average size: 60−150 μm). Various grafted solids were studied, with pore diameter ranging between 4 and 15 nm and organic group contents of typically 1.4−1.9 mmol g^{-1}. Diffusion processes in the porous organically modified silicas were found to be dramatically restricted as compared to those observed in homogeneous solution ($\approx 10^3$−10^4 times slower). They were dependent on several factors such as the pore size of the material and the size of the reactant, the density of grafted organic sites, and the nature of the starting silica gel. Evaluation of apparent diffusion coefficients was achieved by applying a simplified model based on spherical diffusion. This has allowed us to point out a significant decrease in the access rates upon gradual completion of reactions: as the reactant concentration in the vicinity of increasing amounts of grafted groups is raised progressively, there is less room available in the porous structure to enable the probe to reach rapidly the remaining active sites. The apparent diffusion coefficient was found to drop dramatically after typically 30−50% reaction completion, depending on the nature of the probe. This study allows highlighting the optimal conditions that should be required to ensure efficient application of grafted silica gels, that is, in the fields of catalysis or heavy metal extraction.

1. Introduction

Materials made of immobilized reagents in polymeric matrixes have emerged in many fields of chemistry, including heterogeneous catalysis and green chemistry,[1] separation sciences and remediation processes,[2] electrochemistry and sensors,[3] or supramolecular devices.[4] Of special interest are the silica-based organic−inorganic hybrids because they combine the attractive properties of a mechanically and thermally stable inorganic backbone,[5,6] that can be quite easily prepared with a tailor-made structure by means of the versatile sol−gel technique,[7,8] with a specific chemical reactivity that can be tuned by the choice of appropriate organofunctional groups.[9]

Basically, one can distinguish two kinds of hybrids:[10] (1) those characterized by a weak linkage between the organic and inorganic components, such as impregnated or entrapped ligands within the silica structure (class I), and (2) those involving stronger bonding of organofunctional groups to the polysiloxane lattice (class II).

* Corresponding author. Fax: (+33) 3 83 27 54 44. E-mail: walcariu@lcpe.cnrs-nancy.fr.

(1) (a) Yermakov, Y. I.; Kuznetsov, V. A.; Zacharov, V. A. *Catalysis by Supported Complexes*; Elsevier: Amsterdam, 1981. (b) Clark, J. H. *Catalysis of Organic Reactions by Supported Inorganic Reagents*; VCH: New York, 1994. (c) Schubert, U.; Hüsing, N.; Lorentz, A. *Chem. Mater.* **1995**, *7*, 2010. (d) Krebs, J. F.; Borovik, A. S. *J. Am. Chem. Soc.* **1995**, *117*, 10593. (e) Clark, J. H.; Macquarrie, D. K. *Chem. Soc. Rev.* **1996**, *25*, 303. (f) Cornils, B., Herrmann, W. A., Eds.; *Applied Homogeneous Catalysis with Organometallic Compounds, Vol. 2*; VCH: New York, 1997.

(2) (a) Falter, R.; Schöler, H. F. *Fresenius J. Anal. Chem.* **1995**, *353*, 34. (b) Alexandratos, S. D.; Crick, D. W. *Ind. Eng. Chem. Res.* **1996**, *35*, 635. (c) Eiden, R.; Falter, R.; Castro, B. A.; Schöler, H. F. *Fresenius J. Anal. Chem.* **1997**, *357*, 439. (d) Bradshaw, J. S.; Izatt, R. M. *Acc. Chem. Res.* **1997**, *30*, 338. (e) Watson, J. S. *Separation Methods for Waste and Environmental Applications*; Marcel Dekker: New York, 1999. (f) Seneviratne, J.; Cox, J. A. *Talanta* **2000**, *52*, 801.

(3) (a) Murray, R. W. Molecular Design of Electrodes Surfaces. In *Techniques of Chemistry*; Wiley: New York, 1992; Vol. 22. (b) Dave, B. C.; Dunn. B.; Valentine, J. S.; Zink, J. I. *Anal. Chem.* **1994**, *66*, 1120A. (c) Avnir, D. *Acc. Chem. Res.* **1995**, *28*, 328. (d) Kalcher, K.; Kauffmann, J.-M.; Wang, J.; Svancara, I.; Vytras, K.; Neuhold, C.; Yang, Z. *Electroanalysis* **1995**, *7*, 5. (e) Lev, O.; Wu, Z.; Bharathi, S.; Glezer, V.; Modestov, A.; Gun, J.; Rabinovich, L.; Sampath, S. *Chem. Mater.* **1997**, *9*, 2354. (f) Bescher, E.; Mackenzie, J. D. *Mater. Sci. Eng. C* **1998**, *6*, 145. (g) Walcarius, A. *Chem. Mater.* **2001**, *13*, 3351.

(4) Greaves, M. D.; Rotello, V. M. *J. Am. Chem. Soc.* **1997**, *119*, 10569.

(5) Iler, R. K. *The Chemistry of Silica*; Wiley: New York, 1979.

(6) Unger, K. K. *Porous Silica*; Elsevier: Amsterdam, 1979.

(7) Hench, L. L.; West, J. K. *Chem. Rev.* **1990**, *90*, 33.

(8) Brinker, C. J.; Scherer, G. W. *Sol−Gel Science*; Academic Press: San Diego, 1990.

(9) See, for example: (a) Mark, J. E.; Lee, C. Y.-C.; Bianconi, P. A. Hybrid Organic−Inorganic Composites. *ACS Symp. Ser.* **1995**, *585*. (b) Wen, J.; Wilkes, G. L. *Chem. Mater.* **1996**, *8*, 1667. (c) Chujo, Y. *Curr. Opin. Solid State Mater. Sci.* **1996**, *1*, 806.

(10) Sanchez, C.; Ribot, F. *New J. Chem.* **1994**, *18*, 1007.

10.1021/cm021117k CCC: $22.00
Published on Web 05/10/2002

The latter occurs most often via covalent attachment that can be achieved either by postgrafting synthesis (of typically organochlorosilanes or organoalkoxysilanes) on a preformed silica support[11] or by cocondensation of siloxane and organosiloxane precursors.[1c,12] Contrarily to the case of class I, hybrids of class II are less subjected to leaching of the organic species incorporated into the inorganic phases because of the nonhydrolyzable SiC bond in organosiloxanes.[13]

To ensure the effectiveness of the hybrid materials in exploiting the intrinsic reactivity of the organofunctional groups, these moieties must keep their activity upon immobilization, they must be accessible to the external solution, and mass transfer to and from these active sites should be as fast as possible. As highlighted in recent investigations, this is especially important in heterogeneous catalysis for ensuring high efficiency and turnover,[14−16] as well as in removal of toxic substances (especially heavy metals) to improve the performance of remediation processes and environmental containment technologies,[17−23] and also in electrochemical applications for which diffusion is often the rate-determining step.[24,25]

Active materials with catalysts immobilized on solid supports hold definite advantage over homogeneous counterparts because they are easier to handle, retrieve, and recycle (i.e. they can be separated from reaction mixtures by simple filtration), which reduces the environmental impact of a chemical process and improves product purity.[14] Great efforts were directed to produce hybrid materials with enhanced accessibility to the active centers to improve catalysis in liquid-phase reactions.[15,16] The advent of mesoporous silicas, in particular MCM-41,[26] has generated extensive developments in this direction.[16]

Use of porous solids containing anchoring ligands also holds great promise for selective uptake of contaminants.[17] Many investigations were directed to trap heavy metal species by using organically modified silicas. They include class I hybrids made of various ligands impregnated within silica gels,[18] silica-based materials grafted with organic groups containing either amine functions,[19] sulfur, or thiol centers,[20] or even both of them in more complex systems.[21] Interest in surfactant-templated materials for this purpose was also highlighted.[22] Mercaptopropyl-functionalized silicas received considerable attention as heavy metal ion-trapping agents, especially for removal of mercury(II).[20a,b,23] In the particular case of remediation (i.e. removal of heavy metals), it is quite obvious that the efficiency of the process, in terms of capacity and duration, depends on all the factors affecting the transport of adsorbate, for example, the porosity, accessibility to the binding sites, and structure of the adsorbent. Therefore, these factors should be kept in mind when planning a particular application that proceeds under diffusion control, and careful investigation of their effects on the process would help in defining the optimal experimental conditions. Mass transport by diffusion in porous solids also

(11) (a) Vansant, E. F.; Van der Voort, P.; Vrancken, K. C. *Characterisation and Chemical Modification of the Silica Surface*; Elsevier: The Netherlands, 1995. (b) Sentell, K. B.; Bliesner, D. M.; Shearer, S. T. In *Chemically Modified Surfaces*; Pesek, J. J., Leigh, I. E., Eds.; Royal Society of Chemistry: Cambridge, 1994; p 190. (c) Kantipuly, C.; Katragadda, S.; Chow, A.; Gesser, H. D. *Talanta* **1990**, *37*, 491. (d) Unger, K. K., Ed.; *Packings and Stationary Phases in Chromatographic Techniques*; Marcel Dekker: New York, 1990.

(12) (a) Loy, D. A.; Shea, K. J. *Chem. Rev.* **1995**, *95*, 1431. (b) Corriu, R. J. P.; Leclercq, D. *Angew. Chem., Int. Ed. Engl.* **1996**, *35*, 1420. (c) Livage, J. *Curr. Opin. Solid State Mater. Sci.* **1997**, *2*, 132. (d) Hüsing, N.; Schubert, U. *Angew. Chem., Int. Ed. Engl.* **1998**, *37*, 22. (e) Sanchez, C.; Ribot, F.; Lebeau, B. *J. Mater. Chem.* **1999**, *9*, 35.

(13) Mahmoud, M. E.; Osman, M. M.; Amer, M. E. *Anal. Chim. Acta* **2000**, *415*, 33.

(14) (a) Sheppard, E. W.; Zhou, W.; Maschmeyer, T.; Matters, J. M.; Roper, C. L.; Parsons, S.; Johnson, B. F. G.; Duer, M. J. *Angew. Chem., Int. Ed. Engl.* **1998**, *37*, 2719. (b) Maschmeyer, T.; Oldroyd, R. D.; Sankar, G.; Thomas, J. M.; Shannon, I. J.; Klepetko, J. A.; Masters, A. F.; Beattie, J. K.; Catlow, C. R. A. *Angew. Chem., Int. Ed. Engl.* **1997**, *36*, 1639.

(15) (a) Brunel, D.; Cauvel, A.; Fajula, F.; Di Renzo, F. *Stud. Surf. Sci. Catal.* **1995**, *97*, 173. (b) Corma, A. *Chem. Rev.* **1997**, *97*, 2373. (c) Bellocq, N.; Abramson, S.; Lasperas, M.; Brunel, D.; Moreau, P. *Tetrahedron: Asymmetry* **1999**, *10*, 3229. (d) Lim, M. H.; Stein, A. *Chem. Mater.* **1999**, *11*, 3285.

(16) (a) Brunel, D. *Microporous Mesoporous Mater.* **1999**, *27*, 329. (b) Price, P. M.; Clark, J. H.; Macquarrie, D. J. *Dalton* **2000**, 101. (c) Clark, J. H.; Macquarrie, D. J.; Wilson, K. *Stud. Surf. Sci. Catal.* **2000**, *129*, 251.

(17) Cooper, C.; Burch, R. *Water Res.* **1999**, *33*, 3689.

(18) See, for example: (a) Zaporozhets, O.; Gawer, O.; Sukhan, V. *Talanta* **1998**, *46*, 1387. (b) Zaporozhets, O.; Petruniock, N.; Bessarabova, O.; Sukhan, V. *Talanta* **1999**, *49*, 899. (c) Zaporozhets, O.; Gawer, O.; Sukhan, V. *Colloids Surf., A* **1999**, *147*, 273. (d) Singh, R.; Khwaja, A. R.; Gupta, B.; Tandon, S. N. *Talanta* **1999**, *48*, 527.

(19) (a) Kham, K.; Deratani, A.; Sebille, B. *New J. Chem.* **1987**, *11*, 709. (b) Hoorn, H. J.; de Joode, P.; Driessen, W. L.; Reedijk, J. *Recl. Trav. Chim. Pays-Bas* **1996**, *115*, 191. (c) Vieira, E. F. S.; Simoni, J. A.; Airoldi, C. *J. Mater. Chem.* **1997**, *7*, 2249. (d) Bresson, C.; Menu, M.-J.; Dartiguenave, M.; Dartiguenave, Y. *J. Environ. Monit.* **2000**, *2*, 240. (e) Fonseca, M. G.; Oliveira, A. S.; Airoldi, C. *J. Colloid Interface Sci.* **2001**, *240*, 533.

(20) (a) Cestari, A. R.; Airoldi, C. *J. Braz. Chem. Soc.* **1995**, *6*, 291. (b) Cestari, A. R.; Airoldi, C. *J. Colloid Interface Sci.* **1997**, *195*, 338. (c) Dai, S.; Burleigh, M. C.; Shin, Y.; Morrow, C. C.; Barnes, C. E.; Xue, Z. *Angew. Chem., Int. Ed. Engl.* **1999**, *38*, 1235. (d) El-Nahhal, I. M.; Zaggout, F. R.; El-Ashgar, N. M. *Anal. Lett.* **2000**, *33*, 2031. (e) Im, H.-J.; Yang, Y.; Allain, L. R.; Barnes, C. E.; Dai, S.; Xue, Z. *Environ. Sci. Technol.* **2000**, *34*, 2209. (f) Burleigh, M. C.; Dai, S.; Hagaman, E. W.; Lin, J. S. *Chem. Mater.* **2001**, *13*, 2537. (g) Leyden, D. E.; Luttrell, G. H.; Sloan, G. E.; DeAngelis, N. J. *Anal. Chim. Acta* **1976**, *84*, 97. (h) Leyden, D. E.; Luttrell, G. H. *Anal. Chem.* **1975**, *47*, 1612.

(21) (a) Nesterenko, P. N.; Ivanov, A. V.; Galeva, N. A.; Seneveratne, G. B. C. *J. Anal. Chem.* **1997**, *52*, 736. (b) Dias Filho, N. L.; Gushikem, Y. *Sep. Sci. Technol.* **1997**, *32*, 2535. (c) Dias Filho, N. L. *Colloids Surf., A* **1998**, *144*, 219. (d) Mahmoud, M. E. *Anal. Chim. Acta* **1999**, *398*, 297. (e) Broudic, J.-C.; Conocar, O.; Moreau, J. J. E.; Meyer, D.; Wong Chi Man, M. *J. Mater. Chem.* **1999**, *9*, 2283. (f) Ma, W. X.; Liu, F.; Li, K. A.; Chen, W.; Tong, S. Y. *Anal. Chim. Acta* **2000**, *416*, 191. (g) Liu, A. M.; Hidajat, K.; Kawi, S.; Zhao, D. Y. *Chem. Commun.* **2000**, 1145. (h) Soliman, E. M.; Mahmoud, M. E.; Ahmed, S. A. *Talanta* **2001**, *54*, 243. (i) Lee, B.; Kim, Y.; Lee, H.; Yi, J. *Microporous Mesoporous Mater.* **2001**, *50*, 77.

(22) See, for example: (a) Moller, K.; Bein, T. *Chem. Mater.* **1998**, *10*, 2950. (b) Lim, M. H.; Blanford, C. F.; Stein, A. *Chem. Mater.* **1998**, *10*, 467. (c) Diaz, I.; Marquez-Alvarez, C.; Mohino, F.; Perez-Pariente, J.; Sastre, E. *J. Catal.* **2000**, *193*, 283. (d) Margolese, D.; Melero, J. A.; Christiansen, S. C.; Chmelka, B. F.; Stucky, G. D. *Chem. Mater.* **2000**, *12*, 2448.

(23) (a) Feng, X.; Fryxell, G. E.; Wang, L.-Q.; Kim, A. Y.; Liu, J.; Kemmer, K. M. *Science* **1997**, *276*, 923. (b) Mercier, L.; Pinnavaia, T. J. *Adv. Mater.* **1997**, *9*, 500. (c) Mercier, L.; Pinnavaia, T. J. *Environ. Sci. Technol.* **1998**, *32*, 2749. (d) Brown, J.; Mercier, L.; Pinnavaia, T. J. *Chem. Commun.* **1999**, 69. (e) Mattigod, S. V.; Feng, X.; Fryxell, G. E.; Liu, J.; Gong, M. *Sep. Sci. Technol.* **1999**, *34*, 2329. (f) Brown, J.; Richer, R.; Mercier, L. *Microporous Mesoporous Mater.* **2000**, *37*, 41.

(24) (a) Collinson, M. M. *Mikrochim. Acta* **1998**, *129*, 149. (b) Walcarius, A. *Electroanalysis* **1998**, *10*, 1217. (c) Walcarius, A. *Electroanalysis* **2001**, *13*, 701.

(25) (a) Walcarius, A.; Despas, C.; Trens, P.; Hudson, M. J.; Bessière, J. *J. Electroanal. Chem.* **1998**, *453*, 249. (b) Walcarius, A.; Lüthi, N.; Blin, J.-L.; Su, B.-L.; Lamberts, L. *Electrochim. Acta* **1999**, *44*, 4601. (c) Villemure, G.; Pinnavaia, T. J. *Chem. Mater.* **1999**, *11*, 789. (d) Walcarius, A.; Bessière, J. *Chem. Mater.* **1999**, *11*, 3009. (e) Etienne, M.; Bessière, J.; Walcarius, A. *Sens. Actuators, B* **2001**, *76*, 531.

(26) (a) Kresge, C. T.; Leonowicz, M. E.; Roth, W. J.; Vartuli, J. C.; Beck, J. S. *Nature* **1992**, *359*, 710. (b) Beck, J. S.; Vartuli, J. C.; Roth, W. J.; Leonowicz, M. E.; Kresge, C. T.; Schmitt, K. D.; Chu, C. T.-W.; Olson, D. H.; Sheppard, E. W.; McCullen, S. B.; Higgins, J. B.; Schlenker, J. L. *J. Am. Chem. Soc.* **1992**, *114*, 10834.

plays an important role in controlling migration of contaminants in siliceous soils.[27]

Actually, several works are concerned with detailed studies on the accessibility to the active chemical functions in organic−inorganic hybrid materials, and great efforts are focusing on improving their applications in both catalysis and metal ions uptake by producing new materials with increased accessibility.[2f,14a,15c,23,28] Sometimes, the reaction speed was briefly characterized,[13,19d,20d−f,21d,f,29] but thorough and in-depth investigations of mass transfer kinetics to the active sites, for organically modified silica particles suspended in solution, remain uncommon.[19a,23e,30]

The current work addresses the issues of both accessibility and diffusion rates to the binding sites for target reagents in various silica gels grafted with either aminopropyl or mercaptopropyl groups. It presents a detailed study of the main parameters that affect the protonation of aminopropylsilica (APS) and the uptake of model heavy metals by grafted silicas, such as Cu^{II} by APS and Hg^{II} by mercpatopropylsilica (MPS). It was shown that the porosity, the density of the organic ligands, both particle and reactant sizes, and the nature of the starting gel affect to a significant extent the speed of binding processes. Applying a very simple diffusion model to the kinetic studies was shown to be convenient for estimation of apparent diffusion coefficients within the solids. The latter were found to decrease upon filling the material with species liable to interact with the organofunctional groups.

2. Experimental Section

2.1. Materials and Reagents. Silica gel samples of chromatographic grade were purchased from Merck: Geduran SI 60 (G60), Kieselgel 40 (K40), Kieselgel 60 (K60), and Kieselgel 100 (K100). Some of their physicochemical properties are listed in Table 1. The grafting reagents, (3-aminopropyl)triethoxysilane (APTES, 99%, Sigma-Aldrich) and (mercaptopropyl)-trimethoxysilane (MPTMS, 95%, Lancaster) were used without further modification. Toluene (99%) was obtained from Merck and dried before use.

All reagents were analytical grade (Fluka, Prolabo): hydrochloric acid (min. 36%), trifluoroacetic acid (min. 98%), picric acid, ammonia (28−30%), mercury(II) nitrate—*attention, mercury is highly toxic*—and copper(II) nitrate. Acid solutions were standardized using 1.002 M sodium hydroxide (Titrinorm, Prolabo). Buffers were prepared using acetic acid (min. 99.8%, Prolabo) and sodium acetate (min. 99.5%, Prolabo). Solutions were prepared with high-purity water (18 MΩ·cm^{-1}) obtained from a Millipore milliQ water purification system, or in 90:10 ethanol/water mixtures (from ethanol 95−96%, Merck).

Table 1. Physical Characteristics of Starting Silica Gels

	nitrogen adsorption			average particle size[b]	
gel	BET surf area/m^2 g^{-1}	tot pore vol/cm^3 g^{-1}	pore diam[a]/Å	based on no./μm	based on vol/μm
K40	552	1.04	45	151	360
K60	457	0.81	70	111	224
K100	294	0.63	147	138	273
G60	390	0.76	75	70	199

[a] Estimated according to $D = (4V_p/A)$, with D = average pore diameter, V_p = total pore volume, and A = specific surface area, according to ref 46; the pore size distribution is given in the Supporting Information. [b] Determined from cumulative particle size distribution analysis.

2.2. Surface Modification of the Silica Samples. Silica gels functionalized with *n*-propyl-NH_2 or -SH were typically prepared as follows. (Aminopropyl)silica (APS) was obtained by adding 6 mL of APTES to a 50 mL stirred suspension of the starting gel (5 g of either G60, K40, K60, or K100) in refluxing toluene for 2 h. After slow cooling of the mixture, the solid phase was recovered by filtration and washed with fresh toluene. It was then heated at 120 °C during 12 h. Several APS-G60 samples containing various amounts of *n*-propyl-NH_2 groups were also prepared by adjusting in defect the grafting reagent. (Mercaptopropyl)silica (MPS) was synthesized according to a similar procedure using 5 mL of MPTMS (instead of APTES); in this case, however, the reflux under stirring was maintained during 24 h. After filtration and thorough washing with dry toluene, the grafted product was dried overnight under vacuum.

2.3. Characterization of Grafted Materials—Instrumentation. The amount of grafted ligands on both APS and MPS samples was determined by elemental analysis of N or S (Table 2). APS was characterized by acid−base titration at various speeds with the aid of an automated titrator (716 DMS Titrino, Metrohm) associated to the Metrohm 691 pH meter; back-titration from excess of acid was also performed to quantify the loading of materials with amine groups.[31] Metal binding capacities (Cu^{II} on APS and Hg^{II} on MPS) were evaluated by allowing to react typically 100 mg of the solid phase in 50 mL of solution containing the target metal ion at a selected initial concentration, during 2 h (APS) or 24 h (MPS). The reaction time for APS samples was limited to 2 h in order to prevent degradation of silica, which is known to occur in aqueous suspensions in the presence of amine ligands.[32] Analyses of both Cu^{II} and Hg^{II} were performed by inductively coupled plasma−atomic emission spectroscopy (ICP-AES, Plasma 2000, Perkin-Elmer).

Crude silica samples and grafted products were also characterized by various physical methods. BET analysis was performed by measurements of nitrogen adsorption−desorption isotherms, at 77 K in the relative pressure range from about 10^{-5} to 0.99, on a Coulter instrument (model SA 3100). The pore volumes and the external surface areas were obtained by the *t*-plot method.[33] The pore size distribution is reported in the Supporting Information. Particle size was characterized using a light scattering particle size distribution analyzer (model LA920, Horiba), based on the Mie scattering theory. Back diffusion scanning micrographs were obtained with a Philips XL30 scanning electron microscope (SEM).

2.4. Kinetic Experiments: Protonation of Aminopropyl-Grafted Silicas. Protonation kinetics of APS samples by various acids (hydrochloric, trifluoroacetic, or picric) were investigated from batch experiments. A suitable amount of APS (typically 10−100 mg) was suspended in 20−25 mL of pure water and sonicated during 5 s to ensure appropriate

(27) (a) Farrell, J.; Grassian, D.; Jones, M. *Environ. Sci. Technol.* **1999**, *33*, 1237. (b) Werth, C. J.; Reinhard, M. *Environ. Sci. Technol.* **1997**, *31*, 697.

(28) (a) Bossaert, W.; De Vos, D. E.; Van Rhijn, W. M.; Bullen, J.; Grobet, P. J.; Jacobs, P. A. *J. Catal.* **1999**, *182*, 156. (b) Bezombes, J.-P.; Chuit, C.; Corriu, R. J. P.; Reyé, C. *J. Mater. Chem.* **1999**, *9*, 1727. (c) Dubois, G.; Corriu, R. J. P.; Reyé, C.; Brandès, S.; Denat, F.; Guilard, R. *Chem. Commun.* **1999**, 2283. (d) Corriu, R. J. P.; Hoarau, C.; Mehdi, A.; Reyé, C. *Chem. Commun.* **2000**, 71. (e) Bezombes, J.-P.; Chuit, C.; Corriu, R. J. P.; Reyé, C. *Can. J. Chem.* **2000**, *78*, 1519. (f) Kloster, G. M.; Watton, S. P. *Inorg. Chim. Acta* **2000**, *297*, 156. (g) Egelhaaf, H.-J.; Holder, E.; Herman, P.; Mayer, H. A.; Oelkrug, D.; Lindner, E. *J. Mater. Chem.* **2001**, *11*, 2445.

(29) (a) Lakatos, I.; Lakatos-Szabo, J. *Colloids Surf., A* **1998**, *141*, 425. (b) Leventis, N.; Elder, I. A.; Rolison, D. R.; Anderson, M. L.; Merzbacher, C. I. *Chem. Mater.* **1999**, *11*, 2837. (c) Vaton-Chanvrier, L.; Bucaille, N.; Combret, Y.; Combret, J.-C. *J. Liq. Chromatogr. Relat. Technol.* **2000**, *23*, 2155. (d) Badjic, J. D.; Kostic, N. M. *J. Mater. Chem.* **2001**, *11*, 408.

(30) (a) Netrabukkana, R.; Lourvanij, K.; Rorrer, G. L. *Ind. Eng. Chem. Res.* **1996**, *35*, 458. (b) Campos, D. S.; Eic, M.; Occelli, M. L. *Stud. Surf. Sci. Catal.* **2000**, *129*, 639.

(31) Yang, J. J.; El-Nahhal, I. M.; Chuang, I.-S.; Maciel, G. E. *J. Non-Cryst. Solids* **1997**, *209*, 19.

(32) Zhmud, B. V.; Sonnefeld, J. *J. Non-Cryst. Solids* **1996**, *195*, 16.

(33) Lippens, B. C.; de Boer, J. H. *J. Catal.* **1965**, *4*, 319.

Table 2. Physical Characteristics of Silica Gels Grafted with Either Aminopropyl or Mercaptopropyl Groups

	nitrogen adsorption			amount of grafted ligands[b]		average particle size[c]	
sample	BET surf area/$m^2\ g^{-1}$	tot pore vol/$cm^3\ g^{-1}$	pore diam[a]/Å	aminopropyl/ mmol g^{-1}	mercaptopropyl/ mmol g^{-1}	based on no./μm	based on vol/μm
APS-K40	266	0.30	45	1.7		109	184
APS-K60	247	0.42	68	1.8		98	176
APS-K100	211	0.73	138	1.4		101	152
APS-G60	215	0.39	73	1.9		62	89
MPS-K40	355	0.32	36		1.5	78	139
MPS-K60	338	0.47	56		1.5[5]	77	116
MPS-K100	252	0.76	121		1.0[5]	78	116
MPS-G60	314	0.44	56		1.4[5]	63	89

[a] Estimated according to $D = (4V_p/A)$, with D = average pore diameter, V_p = total pore volume, and A = specific surface area, according to ref 46; the pore size distribution is given in the Supporting Information. [b] Expressed per gram of grafted material. [c] Determined from cumulative particle size distribution analysis.

dispersion of the solid particles into the solution. An accurate amount of acid solution at a selected well-known concentration was added in the slurry under constant stirring, and pH was monitored continuously as time evolved. One pH value was recorded every 0.25 s by means of homemade software, using a Metrohm 691 pH-meter (with glass electrode Metrohm N*o*. 6.0222.100). The increase in pH was used to quantify the consumption of protons. Calibration was performed from non-proton-consuming pure silica gel suspensions (see Supporting Information for details, Figure A). The error on the measurement of proton uptake is estimated to be less than 5%.

2.5. Kinetic Experiments: Adsorption of Mercury(II) and Copper(II) on Mercaptopropyl- and Aminopropyl-Grafted Silicas. The rates of uptake of Hg^{II} by MPS and that of Cu^{II} by APS are much less rapid than protonation of APS materials, so that their characterization does not require absolutely a continuous monitoring of the solution-phase composition and intermittent measurements would be quite satisfactory. Typical batch experiments were carried out by dispersing selected amounts of solid material (typically 50 mg of either APS or MPS) into several solutions (50 mL) containing either Cu^{II} or Hg^{II} at an appropriate initial concentration. After selected periods of time, ranging from 1 min to several hours, the remaining metal concentrations in solution were determined quantitatively to allow calculation of the amounts of adsorbed species on the solid phases by difference with respect to the starting concentrations. At this time, the concentrations of copper(II) in solution were determined by ICP-AES while those of mercury(II) required a more sensitive method based on complexation by dithizone, extraction of the resulting complex in CCl_4, and UV detection at 490 nm[34] (spectrometer Beckmann DU 7500).

2.6. Kinetic Data Treatment. Most often, the results of kinetic experiments were presented in the form of plots giving the evolution of Q/Q_0 ratios versus time, where Q is the amount of reactant (analyte) that has reached the binding sites within/on the solid particles at time t, and Q_0 is the maximum of accessible binding sites for the target analyte species (that is the amount of analyte within/on the solid at time = ∞). Q/Q_0 is therefore equal to zero at $t = 0$ and to unity after completion of the reaction. Variation of Q/Q_0 with time is thus a direct indication of the binding rate of the analyte species to the organic ligands grafted to the various silica structures (acids or Cu^{II} on APS and Hg^{II} on MPS).

As diffusion of reactants within the porous structure of APS and MPS can be considered as the rate-determining step of the binding process, these curves were fitted according to a non-steady-state diffusion model. In view of the rather high heterogeneity of particle morphologies, which cannot be taken into account in a simple model, the solid particles were considered as spherical in a first approximation. This approximation appears to be acceptable to compare the behavior of the various grafted silicas between them, as their respective particle shapes did not differ significantly from each other (all look like "gravels"; none of them display regular shapes such as cylinders, cones, sheets, tubes, or anything else). Diffusion in a sphere is given by eq 1:[35]

$$\frac{Q}{Q_0} = 6\left(\frac{Dt}{a^2}\right)^{1/2}\left\{\pi^{-1/2} + 2\sum_{n=1}^{\infty}(-1)^n \operatorname{ierfc}\frac{na}{\sqrt{Dt}}\right\} - 3\frac{Dt}{a^2} \quad (1)$$

where Q/Q_0 has been defined above, D is the apparent diffusion coefficient, a is the particle size radius, ierfc is the error function, and t is time. Knowing particle size allows us to estimate the apparent diffusion coefficients by appropriate fitting of the experimental curve Q/Q_0 versus t.

This model is intrinsically valid for a homogeneous sample of spheres of monodisperse size. The grafted silica samples, however, do exist under a relatively wide particle size distribution, so that the overall curve Q/Q_0 versus t would be the level-headed sum of each contribution of populations displaying the same particle size a_x (eq 2).

$$\frac{Q}{Q_0} = \sum_{x=1}^{x=n} f_{a_x}\left[6\left(\frac{Dt}{a_x^2}\right)^{1/2}\left\{\pi^{-1/2} + 2\sum_{n=1}^{\infty}(-1)^n \operatorname{ierfc}\frac{na_x}{\sqrt{Dt}}\right\} - 3\frac{Dt}{a_x^2}\right] \quad (2)$$

where f_{a_x} is the relative fraction of particles having the same size a_x; this fraction ranges from 0 to 1 and is determined from particle size distribution measurements. For samples made of particles with various sizes, equivalence between eqs 1 and 2 can be achieved by calculating the average particle size based on volume (see Supporting Information).

3. Results and Discussion

3.1. Protonation of Aminopropyl-Grafted Mesoporous Silicas. Comparing the data of Tables 1 and 2 highlights the effects of grafting silica gels with APTES on the physical characteristics of materials. As expected, both specific surface area and pore volume decreased upon grafting, and the extent of change was higher for materials with lower pore size. This is due to the aminopropyl chains occupying some space in the material. Also, the particle size of grafted solids was smaller than that of the starting gels, as explained by attrition as a consequence of mechanical stirring during synthesis. The amount of amine groups linked to the silica structure was dependent on both the type and porosity of the starting gel, resulting in higher loading in APS-G60 with respect to APS-K60, while increasing site densities were observed in the Kieselgel series from APS-K40 to APS-K100 (1.9, 2.4, and 2.9 groups per

(34) Meites, L. *Handbook of Analytical Chemistry*; McGraw-Hill: New York, 1963.

(35) Crank, J. *The Mathematics of Diffusion*; Clarendon Press: Oxford, 1975.

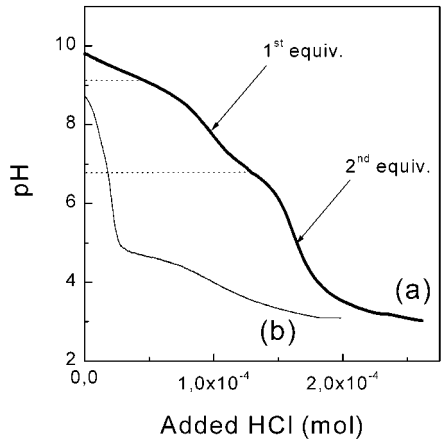

Figure 1. Titration curves for 100.6 mg of APS-G60 in 50 mL of 0.0104 M HCl solution: (a) 0.03 mL min^{-1}; (b) 1.00 mL min^{-1}.

square nanometer, respectively, for APS-K40, APS-K60, and APS-K100). This agrees well with higher accessibility to the silica surface in more open structures.[36]

APS samples are intrinsically basic because of their grafted amine groups. Figure 1 (curve a) shows a typical titration curve, recorded by adding the acid slowly enough to ensure quantitative protonation of all NH_2 groups. It exhibits two successive jumps that can be assigned respectively to the protonation of "free" amine (eq 3) and to that of the zwitterion-like species,

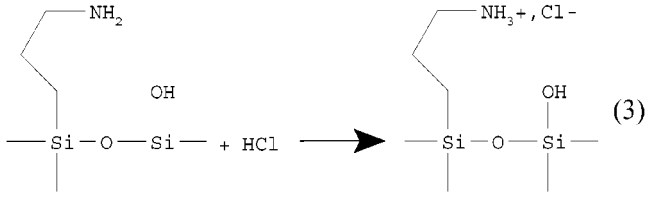

(3)

$\equiv RNH_3^{+-}OSi\equiv$, (eq 4) that is known to occur when

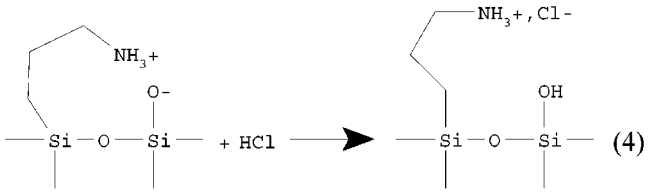

(4)

(aminopropyl)silica is contacting an aqueous medium.[32] The first step is characterized by an apparent pK_a above 9 and includes most probably, at least in part, the protonation of solution-phase amine moieties arising from the alkaline degradation of APS in water.[37] The second step is consistent with protonation of silanolate groups, SiO^-, in agreement with the intrinsic pK_a values reported for surface silanol groups (pK_a = 6.8 ± 0.2, as determined by Schindler and Kamber[38] at 25 °C in 0.1 M $NaClO_4$). The ratio between $\equiv RNH_2$ and $\equiv RNH_3^{+-}OSi\equiv$ species is close to 60:40, independent of the amount of amine groups grafted on silica gel (in the 0.3−2.2 mmol g^{-1} range). Confinement of $\equiv RNH_2$ groups within the silica matrix promotes the formation of the zwitterion, as compared to the free APTES compound, which is known to form octamers in aqueous medium, resulting in a $\equiv RNH_2$ to $\equiv RNH_3^{+-}OSi\equiv$ ratio of 92%, as revealed by acid−base titration.[39] Zwitterion species are less subjected to leaching in solution as compared to the isolated aminopropyl groups because NH_2 is less available to attack the silica surface.[11a,32]

When increasing significantly the titration speed, the protonation yield drops dramatically (Figure 1, curve b). In this case, protons are only liable to react with $\equiv RNH_2$ groups that are located at the outermost surface of APS particles or with those being lost in the medium at the time scale of the experiment (less than 15%), while the excess accumulates in the external solution. More time is required to ensure quantitative protonation of the internal alkaline moieties. This constitutes the basis of kinetic studies discussed hereafter. By injecting directly a selected amount of acid into an aqueous suspension of APS, the continuous pH monitoring as a function of time is indicative of the speed of the protonation process.

Typical kinetic curves are depicted in Figure 2A for various initial acid to $\equiv RNH_2$ concentration ratios. Lower ratios gave rise to faster proton consumption. This is indicative of diffusional limitations that become more critical as the reaction evolves. Indeed, low amounts of protons are rapidly consumed by reacting with amine groups located in the outer shell of APS particles, while higher amounts have also to reach the reactive centers located deeper in the bulk material. For example, protonation of the 40% most accessible amine groups was achieved in less than 5 min while 100% reaction required more than 5 h. Interestingly, a presentation of data with respect to the total amount of amine groups in the material, as a function of square root of time, reveals a rather nice superimposition of curves up to 50% filling (Figure 2A, inset). This indicates diffusional limitations of the same order of magnitude in the first half of reaction progress, as the slope of such Q/Q_0 versus $\sqrt{t}$ plots is directly related to the apparent diffusion coefficient.[35] Note that experimental data recorded at very short time are overestimated because they correspond to reaction of amine groups that have leached out of the material and therefore did not participate in the restricted diffusion in the porous solid (protons react with them immediately in solution). This is especially visible in Figure 2A (inset) for the H^+/NH_2 ratio of 20% and, to a lesser extent, for the 40% ratio.

Fitting the experimental Q/Q_0 versus t plots, according to a simple model of diffusion in a sphere[35] (eq 1), enables us to estimate the evolution of the apparent diffusion coefficient, D_{app}, as long as protonation evolves (Figure 2B). This coefficient is considered as *apparent* because it includes at one and the same time transport of both protons and counterions (Cl^- in this case) to respectively the amine and corresponding ammonium groups (eqs 3 and 4). Values have been calculated by taking into account the average size of APS samples as they were used in kinetic experiments. During the first half of the reaction, D_{app} is nearly constant (decreasing slowly from 1.4 to 1.3 × 10^{-8} cm^2 s^{-1}), while dropping

(36) Vrancken, K. C.; Van der Voort, P.; Possemiers, K.; Vansant, E. F. *J. Colloid Interface Sci.* **1995**, *174*, 86.
(37) Etienne, M.; Bessière, J.; Walcarius, A. Manuscript in preparation.
(38) Schindler, P.; Kamber, H. R. *Helv. Chim. Acta* **1968**, *51*, 1781.
(39) Coche-Guérente, L.; Desprez, V.; Labbé, P. *J. Electroanal. Chem.* **1998**, *458*, 73.

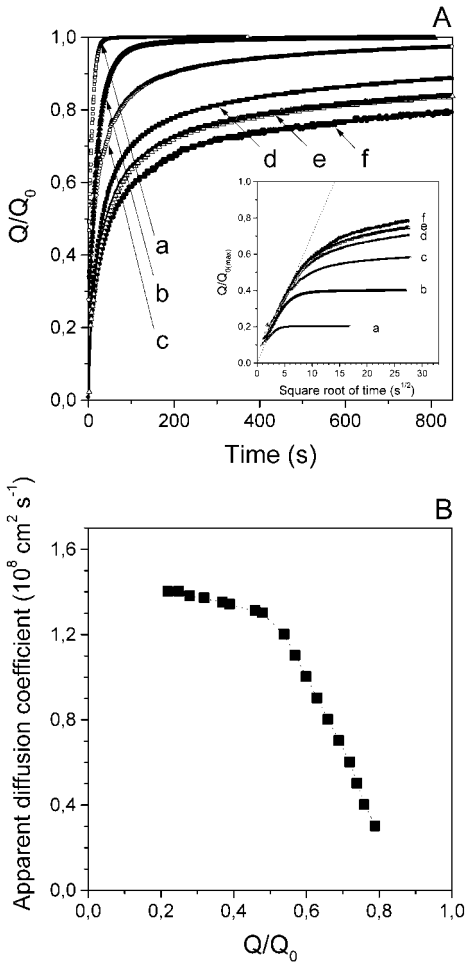

Figure 2. (A) Protonation kinetics for APS-G60 (10 mg) in 25 mL of HCl solutions. The initial concentration of protons was adjusted to get various H^+/RNH_2 ratios: (a) 20%; (b) 40%; (c) 60%; (d) 80%; (e) 90%; (f) 100%. $Q_0 = 1$ is defined with respect to the initial amount of protons (that is the maximum amount of RNH_2 groups that can be protonated), while Q is the amount of protonated RNH_2 groups ($RNH_3^+Cl^-$). Inset: Same data expressed according to the evolution of $Q/Q_{0(max)}$ as a function of square root of time, where $Q_{0(max)}$ represents the total amount of RNH_2 groups on the APS-G60 material. (B) Variation of the apparent diffusion coefficient during protonation as a function of the extent of reaction.

significantly afterward to reach about 20% of its initial value at 80% extent of protonation. Such a decrease can be assigned to restricted access to the amine groups located in small pores of the hybrid structures. Fast and slow sorption/desorption processes have already been reported in silica systems and explained by the difference in the diffusion rates in the mesopores and micropores.[27,40] Diffusion processes are also hindered upon reaction progress, leading to a gradual increase of the amount of $\equiv RNH_3^+,Cl^-$ groups in the porous solid. The presence of these groups in increasing concentration causes progressive pore filling, allotting less space for the reactants to clear a way in the material to reach the remaining unreacted groups. This agrees well with a decrease in the total pore volume that was experimentally observed (N_2 adsorption) when passing from unprotonated APS to the corresponding $\equiv RNH_3^+,Cl^-$ material.

(40) Wirth, M. J.; Swinton, D. J. *Anal. Chem.* **1998**, *70*, 5264.

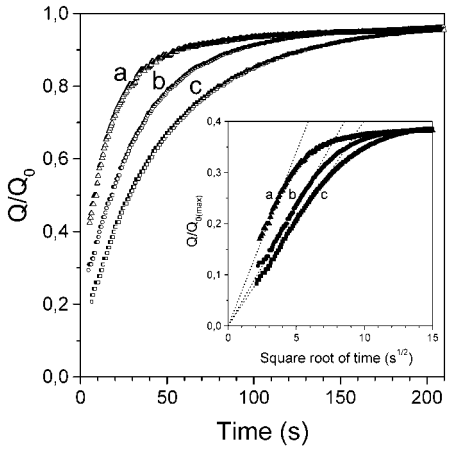

Figure 3. Evolution of protonation kinetics for APS-G60 in HCl solutions (25 mL at the initial concentration of 3.2×10^{-4} M) as a function of the amine content grafted on the material. The amounts of suspended matter in the cell were chosen to ensure a constant H^+/RNH_2 ratio: (a) 25.2 mg of APS-G60 with 0.8 mmol g^{-1} of NH_2; (b) 14.5 mg of APS-G60 with 1.4 mmol g^{-1} of NH_2; (c) 10.0 mg of APS-G60 with 2.1 mmol g^{-1} of NH_2. Inset: same data presented as in Figure 2.

Of course the spherical diffusion model is an oversimplified view of the reality because APS particles are not perfectly spherical and the spatial distribution of NH_2 groups in the structure is most probably not uniform, as previously reported for grafted materials.[15d] Anyway, this approach is rather satisfactory as a first approximation of diffusion-controlled reactions in a so complex heterogeneous system. Its validity was otherwise pointed out by analyzing kinetic data obtained with the same APS sample before and after selected grinding times: similar D_{app} values were calculated by fitting the experimental Q/Q_0 versus t curves recorded for particles of the same nature but displaying different size distributions. It is also interesting to notice that the D_{app} values given by the model at the early stage of reaction are more than 1000 times lower than those of reactants in solution, which supports strong diffusional limitations in the interior of APS particles. The D_{app} values evaluated here are in agreement with literature data: that is, the average diffusion coefficients of quaternary ammonium salts in silica gel (average pore size, 75 Å; pore volume, 0.4−0.5 $cm^3\ g^{-1}$) have been reported to be about 1×10^{-8} $cm^2\ s^{-1}$ using a batch uptake method.[41] As constraints to mass transport are nearly constant during the first half of the reaction (only 7% decrease in D_{app}), the factors affecting protonation of APS materials were studied hereafter in this range ($H^+/\equiv RNH_2$ ratio < 50%).

The effect of amine content on APS protonation kinetics was investigated either at a constant $H^+/\equiv RNH_2$ ratio of 42% by adapting the solid-to-solution ratio in the suspension or at various $H^+/\equiv RNH_2$ ratios with the same solid-to-solution ratio equal to unity. In the first case, the reaction speed was higher with materials containing lower amounts of amine groups (Figure 3). D_{app} values of 2.7×10^{-8}, 1.5×10^{-81}, and 1.0×10^{-8} $cm^2\ s^{-1}$ were evaluated for APS-G60 containing 0.8, 1.4, and 2.1 mmol of $\equiv RNH_2$ per gram, respec-

(41) Ghosh, A. C.; Satyanarayana, K.; Srivastava, R. C.; Dutta, N. N. *Colloids Surf., A* **1995**, *96*, 219.

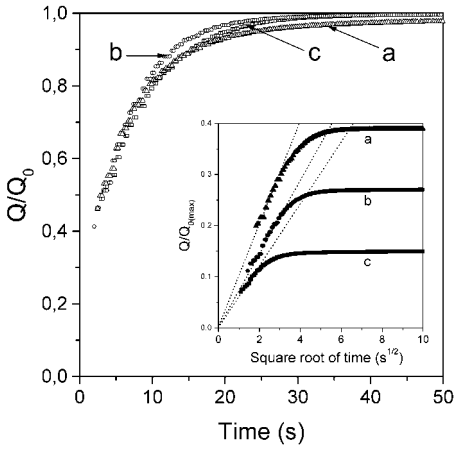

Figure 4. Evolution of protonation kinetics for 25 mg of APS-G60 in HCl solutions (25 mL at the initial concentration of 3.2×10^{-4} M) as a function of the amine content grafted on the material: (a) 0.8 mmol g^{-1}; (b) 1.4 mmol g^{-1}; (c) 2.1 mmol g^{-1}. Inset: same data presented as in Figure 2.

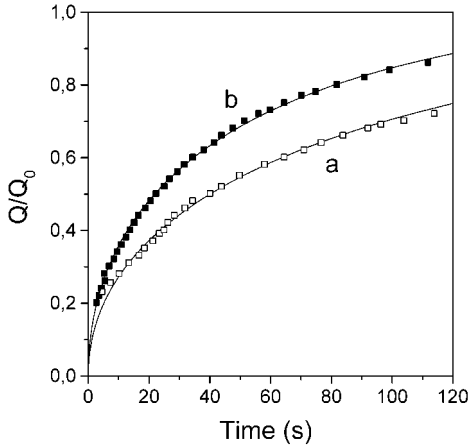

Figure 5. Protonation kinetics for 10 mg of (a) APS-K60 (with 1.91 mmol g^{-1} of NH_2) and (b) APS-G60 (with 1.93 mmol g^{-1} of NH_2) in 25 mL HCl solutions at the initial concentration of 3.2×10^{-4} M (this corresponds to a H^+/RNH_2 ratio of 42%). Inset: same data presented as in Figure 2.

tively. This can be rationalized by considering that higher densities of $\equiv RNH_2$ groups would occupy more places in the APS structure (as otherwise demonstrated by BET analysis) and would therefore contribute to lowering the diffusion rates of protons and associated chloride ions. Another possible contribution could be related to nonrandom coverage of the silica surface by grafted groups (which is liable to occur, especially when prepared in defect): in this case, a major part of the amine groups is probably located at the entrance of the porosity and therefore more rapidly accessible to protons.

On the other hand, consumption of protons looks identical (Figure 4) when working at constant solid-to-solution ratio, and therefore variable $H^+/\equiv RNH_2$ ratios (higher mass of APS containing less $\equiv RNH_2$), but careful analysis of the data with respect to the total amount of amine groups reveals significant differences (Figure 4, inset) that are very close to those observed in Figure 3 (inset). Fitting the curves gave very similar values of D_{app}: 2.8×10^{-8}, 1.7×10^{-8}, and 1.1×10^{-8} $cm^2\ s^{-1}$, respectively, for APS-G60 containing 0.8, 1.4, and 2.1 mmol of $\equiv RNH_2$ per gram. The nearly identical speed of consumption of the same quantity of protons observed in Figure 4 is then explained by a combination of slow diffusion processes in a small thickness of highly loaded APS (2.1 mmol of $\equiv RNH_2\ g^{-1}$) which is counterbalanced by faster diffusion on a larger length scale in APS particles containing lower amounts of $\equiv RNH_2$ groups (0.8 mmol g^{-1}). Reaction of the same amount of protons requires filling a larger volume of APS particles containing few amine groups; on the opposite side, APS samples of higher density of reactive sites would allow quantitative proton consumption by $\equiv RNH_2$ groups situated in a rather narrow shell at the particle boundary. Diffusion processes are therefore controlled by the density of binding sites in the APS sample, and probably also by the heterogeneous coverage of amine groups on the material, but the overall speed of consumption of protons can be monitored by adapting the initial $H^+/\equiv RNH_2$ ratio.

The nature of the starting silica gel was also found to affect the protonation kinetics of APS. This is illustrated in Figure 5, where two different samples displaying approximately the same pore size and very similar amounts of grafted amine groups are compared. This figure also depicts both experimental data and model fitting, illustrating the rather good agreement between them. From experiments carried out at an initial $H^+/\equiv RNH_2$ ratio of 42%, proton consumption was faster with APS-G60 than with APS-K60 (Figure 5), but it should be recalled that the APS-G60 sample was characterized by an average particle size smaller than that for APS-K60 (Table 2). Taking this into account, modelization gave rise to D_{app} values of 1.8×10^{-8} and 1.3×10^{-8} $cm^2\ s^{-1}$, respectively, for APS-K60 and APS-G60. Such a (small) variation cannot be explained by any significant difference in the pore size of the materials (that are very similar and even slightly in favor of APS-G60, see Table 2) but is rather related to the intrinsic differences between these two materials. Indeed, though displaying very similar $\equiv RNH_2$ loadings (per gram of solid), they were characterized by different site densities of 2.4 and 2.9 groups per square nanometer, respectively, for APS-K60 and APS-G60. It is therefore reasonable to ascribe the lower diffusivities to the higher site densities in the APS materials.

Finally, the pore size of APS materials was found to affect protonation kinetics by modulating the speed of diffusion processes in the porous structure. This has been investigated with grafted materials of the Kieselgel series. As expected, the most open structures gave rise to enhanced reaction speeds as compared to those for solids with smaller pore sizes (Figure 6). Fitting data with the spherical diffusion model allows estimating D_{app} values equal to 2.4×10^{-8}, 3.3×10^{-8}, and 5.2×10^{-8} $cm^2\ s^{-1}$, respectively, for APS-K40, APS-K60, and APS-K100. Solvent did not significantly affect protonation kinetics. When performing the same experiments as those depicted in Figure 6, in ethanol, very similar results were recorded and calculation of D_{app} led to values close to those obtained from measurements in aqueous medium: 2.5×10^{-8}, 3.3×10^{-8}, and 4.9×10^{-8} $cm^2\ s^{-1}$, respectively, for APS-K40, APS-K60, and APS-K100. Solvation seems not to play an important role in the rate of access of HCl to the grafted amine groups.

On the opposite hand, the size of the charge-compensating anion influences both the accessibility of

Table 3. Accessibility and Diffusion Rates for Three Acids Reacting with Amine Groups Grafted on Silica Gels Displaying Various Pore Sizes

	percent of $\equiv RNH_2$ groups accessible to:			apparent diffusion coefficient ($\times 10^{-8}$ cm^2 s^{-1}) of:		
material	hydrochloric acid	trifluoroacetic acid	picric acid	hydrochloric acid	trifluoroacetic acid	picric acid
APS-K40	100	91	79	2.4	2.0	1.6
APS-K60	100	100	90	3.3	2.4	2.1
APS-K100	100	100	100	5.2	3.5	3.3

Accessibility was measured from 0.1 g APS suspended in 25 mL solution containing an excess of acid (≈ 120%). Diffusion coefficients were determined at 42% extent of the protonation reaction.

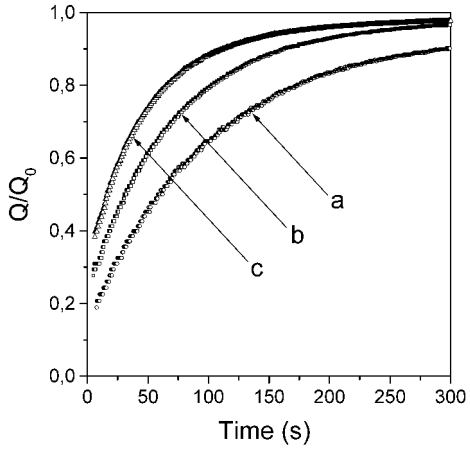

Figure 6. Influence of pore size on the protonation kinetics of various APS samples by HCl: (a) APS-K40 (45 Å); (b) APS-K60 (68 Å); (c) APS-K100 (138 Å); the solid/liquid ratio was adjusted to maintain a constant H^+/RNH_2 ratio of 45%.

protons to the active sites and diffusion rates (Table 3). As protonation of amine groups involves concomitant charge compensation by the counterions associated to protons (eqs 3 and 4), and as the active groups are physically attached inside a porous structure, it is expected that the size of reactants could contribute to affect the reaction efficiency. If 100% protonation yield was observed using HCl independently on the APS sample, uncompleted reactions were evidenced when using strong acids containing bigger associated anions such as trifluoroacetate or picrate (Table 3). Such limitations were stronger with the larger charge-compensating ions. They are clearly due to steric hindrance preventing the amine groups located in small pores from being protonated, as the resulting ammonium moieties cannot be reached by the large anion. At the same time, stronger diffusional limitations were encountered when passing from HCl to trifluoroacetic acid and then to picric acid, as evidenced by measuring protonation kinetics and calculating the corresponding apparent diffusion coefficients (Table 3). The order of magnitude of this effect was nearly the same for all APS samples. Once again, diffusion of large species in a porous medium is much more restricted than that of smaller reactants, as previously reported for metal species in minerals,[42] for sugars in porous silicates or aluminosilicates,[30a] or for cationic dyes in silica gel.[43]

3.2. Adsorption of Mercury on Mercaptopropyl-Grafted Silicas. Mercury(II) is known to react with silica-based materials containing thiol groups covalently linked to the siloxane backbone, to form very stable immobilized complexes.[20a,b,23] It has been reported to have a 1:1 stoichiometry and was used to probe the accessibility of SH groups in new hybrid structures.[23] Four mercaptopropyl silicas (MPSs) were evaluated with respect to their binding ability toward Hg^{II} species in solution. Upon grafting, the MPS samples were characterized by lower porosity as compared to those of the starting silica gels (Table 2). The particle size was also smaller as a result of attrition during the grafting process, and this effect was more intense than that observed for APS samples because synthesis of MPS required more time. Fixation of Hg^{II} was independent of pH in the 1−10 range while a slight capacity decrease was observed at higher pH (i.e. 12), most probably because of partial degradation of the silica material in alkaline medium. Hg^{II} binding to MPS was very stable: no measurable leaching was observed after maintaining a fully Hg^{II}-loaded MPS sample in water during 38 days. As expected from the strong interaction between Hg^{II} and thiol, desorption was not easy. Typically, less than 2% was recovered after 24 h in a HNO_3 + $NaNO_3$ mixture (0.1 M), about 20% in either 2.5 M HCl or 0.1 M KSCN, and 85% in a strong complexing medium containing thiourea (5%) and HCl (0.1 M).

Depending on the material, the percentage of thiol groups accessible to Hg^{II} species was not constant. From experiments performed with 2-fold excess mercury in solution with respect to the amount of thiol in MPS, accessibilities of 57%, 87%, 90%, and 95% were respectively obtained using MPS-K40, MPS-K60, MPS-G60, and MPS-K100. This indicates easier access in the more open structures while some SH groups located in the smallest pores of the less porous materials are not liable to be reached by the reactant. Despite the amorphous nature of the MPS samples, the experimentally observed accessibilities were rather high, at least if compared to the 7% value reported previously for another silica gel (pore size, 40 Å; specific surface area, 750 m^2 g^{-1}) grafted with aminopropyl groups.[23b] This emphasizes the importance of both the nature and the structure of the starting material on the performance of the corresponding grafted solid for metal ion binding. Note that the formation of a Hg^{II}−thiol complex was also exploited for the determination of accessible SH groups in other systems, that is, of biological importance, such as ovalbumin.[44] The main limitation of such an approach is the possible formation of disulfide moieties (that are not complexing Hg^{II}), but they were not evidenced here, at least on the time scale of the experiments.

The rate at which Hg^{II} species reach the binding sites was also a function of the type and porosity of the MPS

(42) Sparks, D. L.; Scheidegger, A. M.; Strawn, D. G.; Scheckel, K. G. In *Mineral-Water Interfacial Reactions, Kinetics and Mechanisms*; Sparks, D. L., Grundl, T. J., Eds.; ACS Symposium Series 715; American Chemical Society: Washington, DC, 1998; Chapter 7.

(43) Nakatani, K.; Sekine, T. *Langmuir* **2000**, *16*, 9256.

(44) Bramanti, E.; D'Ulivo, A.; Lampugnani, L.; Raspi, G.; Zamboni, R. *J. Anal. At. Spectrom.* **1999**, *14*, 179.

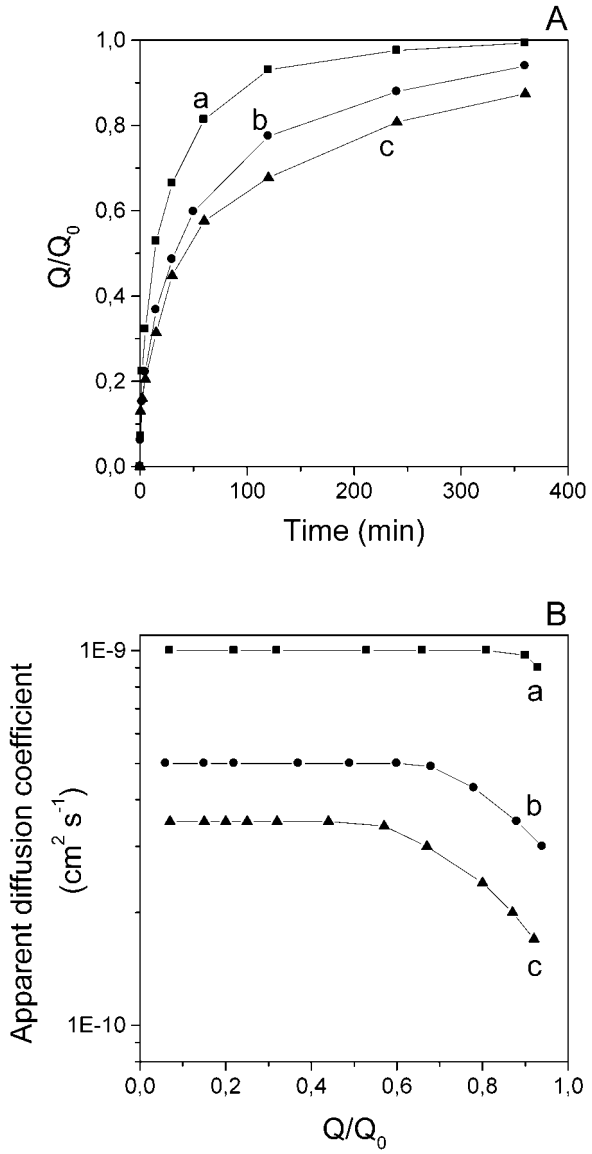

Figure 7. (A) Uptake of Hg(II), as a function of time, by (a) MPS-K100, (b) MPS-K60, and (c) MPS-K40 from a 1.05×10^{-4} M $Hg(NO_3)_2$ solution (in 0.5 M HCl); Hg(II) was in excess with respect to the SH groups; Q_0 is the maximum amount of accessible SH groups. (B) Evolution of the corresponding apparent diffusion coefficients as a function of the extent of the binding process, for (a) MPS-K100, (b) MPS-K60, and (c) MPS-K40.

sample. Similarly to the case of protonation of APS, the rate of fixation of Hg^{II} within MPS was faster when the pore size was bigger (Figure 7A) and/or the amount of reactive groups on the material was lower. Nevertheless, the apparent diffusion coefficients estimated from the same spherical model were significantly smaller than those corresponding to protonation. The values of D_{app} calculated for Hg^{II} in the first stage of the binding process were equal to 3.5×10^{-10}, 5×10^{-10}, and 10×10^{-10} cm^2 s^{-1}, respectively, for MPS-K40, MPS-K60, and MPS-K100. These values are much lower than those reported for diffusion of glucose and related compounds in silica gels of the same porosity.[30a] This difference supports strong interactions between Hg^{II} and MPS, in agreement with the high stability of the S−Hg linkage and the particular affinity of Hg^{II} for the silica surface.[25d] Note that hydrophobicity induced by the mercaptopropyl groups can also contribute to lowering the ingress of aqueous solutions in these materials. As the Hg^{II} uptake goes forward, the material becomes progressively loaded with more and more Hg^{II} species anchored by the thiol groups, and less space is available for diffusion of the metal ion to the remaining binding sites. This results in slowing down the binding process, as highlighted by D_{app} values that are dropping away when filling up the MPS materials (Figure 7B). These stronger diffusional limitations, however, appeared more rapidly in the less porous structure than in the more open materials: drops in D_{app} were observed at about 50%, 65%, and 85% loadings, respectively, for MPS-K40, MPS-K60, and MPS-K100.

The results obtained for the uptake of Hg^{II} by MPS follow the same trends as those that have been pointed out for the protonation of APS, so that it is highly probable that the same factors are affecting both accessibility to the active sites and diffusion rates within the hybrid material, with stronger diffusional limitations with larger reactive probes. Further arguments in that sense will be provided by considering briefly the uptake of Cu^{II} by APS.

3.3. Adsorption of Copper on Aminopropyl-Grafted Silicas in Ethanol. Copper(II) is liable to be immobilized on APS via complexation with the grafted amine groups, as evidenced by the blue color of the resulting solid, most probably in the coordination form involving one amine group, three silanol moieties, and two water molecules.[45] This reaction, when occurring in aqueous medium, is pH dependent and not quantitative (i.e. 4% completion at pH 4.6 and only 34% as the maximum amount obtained at floating pH). Moreover, the lack of stability of APS in aqueous solutions (nonacidic) prevents the application of long equilibration times in the pH range where adsorption occurs, which would be useful to investigate the adsorption kinetics. On the contrary, APS is much more stable in ethanol than in water,[37] and its ability to bind Cu^{II} species is also enhanced (58% completion on the basis of a 1:1 complex). The adsorption kinetics of Cu^{II} on APS were then studied in ethanol, as illustrated in Figure 8 for a typical case. As the overall reaction is not quantitative, one cannot discuss the question of the accessibility to the binding sites. The apparent diffusion coefficient calculated in the early stage of the reaction was about 6×10^{-9} cm^2 s^{-1}, a value 3−4 times lower than that corresponding to the protonation of APS by HCl. This difference is due to the bigger size of Cu^{2+} relative to H^+. Note that accumulation of Cu^{II} within APS also involves diffusion of two charge-compensating anions to neutralize the two positive charge of copper in the material. This probably explains why the apparent diffusion coefficient dropped more rapidly when the reaction went on further, as shown in the inset of Figure 8. Similar constraints were observed for Cu^{II} binding to porous silicas grafted with polyamines of various size, where the fixation rate decreased with the length of the grafted chain.[19a] The factors affecting the rate of access

(45) Klonkowski, A. M.; Grobelna, B.; Widernik, T.; Jankowska-Frydel, A.; Mozgawa, W. *Langmuir* **1999**, *15*, 5814.
(46) Gregg, S. J.; Sing, K. S. W. *Adsorption, Surface Area and Porosity*; Academic Press: London, 1982; pp 113−120.

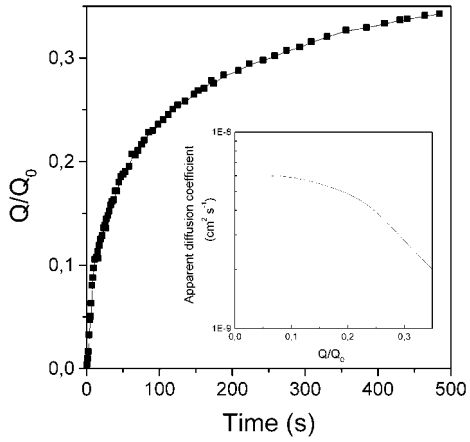

Figure 8. Uptake of Cu(II) by APS-K60 (61 mg) as a function of time, from a 1.0×10^{-3} M $Cu(NO_3)_2$ solution (ethanol/water 90:10); Hg(II) was in excess with respect to the NH_2 groups; Q_0 is the maximum amount of accessible NH_2 groups. Inset: evolution of the corresponding apparent diffusion coefficient during the binding process.

of Cu^{II} in APS samples are of the same nature as those influencing the binding of Hg^{II} to MPS materials.

4. Conclusions

In organically modified silica gels, both accessibility to the reactive centers and (especially) the rate of access to these active sites are dependent on the structural characteristics of the starting silica samples on which organic ligands have been grafted. As demonstrated for protonation of APS and adsorption of some model heavy metals on either MPS or APS, diffusion of reactants in the porous material is the rate-determining step. Diffusion processes were found to be faster in materials displaying larger pore sizes, lower amounts of grafted groups, and smaller particle sizes. By applying a simplified diffusion model, the apparent diffusion coefficients can be evaluated. They were much lower (1000−10000 times) than those generally observed in homogeneous solutions, and they were found to dramatically decrease upon progressive filling of the internal volume of the porous material. This work emphasizes the crucial role played by the starting substrate on the performance of the resulting grafted solid. Further work is currently in progress with grafted crystalline mesoporous silicas to assess the effect of the regular framework on the speed of access to the reactive sites.

Supporting Information Available: Experimental data and figures (PDF). This material is available free of charge via the Internet at http://pubs.acs.org.

Acknowledgment. J. Cortot is gratefully acknowledged for ICP-AES measurements and A. Kohler for SEM images. We also thank the "Service Central d'Analyse" of the CNRS (Lyon) for elemental analyses.

CM021117K